Acoustic Performance of Co- and Counter-Rotating Synchronized Propellers

Burak Turhan*, Hasan Kamliya Jawahar†, Abhishek Gautam‡, Djamel Rezgui§, and Mahdi Azarpeyvand¶
University of Bristol, Queen's Building, Bristol, BS8 1TR, United Kingdom

The understanding and reduction of noise from the new generation of electric propeller-driven aircraft, such as those adopted in Electric Distributed Propulsion (DEP) configurations, is becoming of great importance to the success of these concepts. The study presented in this paper aims to explore the noise suppression capabilities of DEP systems by changing rotation direction and separation distance under both static thrust and in-flow conditions through the implementation of electronic synchronization of the propellers. The noise characteristics of two-bladed propellers were analyzed by conducting experimental measurements on two adjacent, electronically synchronized propellers. The acoustic tests were conducted in an aeroacoustic wind tunnel, using a bespoke rig resembling a DEP system. The experiments involved varying the relative phase angles between the two propellers from 0° to 90°. Each propeller had a diameter of 9 inches and a pitch of 5 inches, operating at a constant rotational speed of 5000 rpm. The noise measurements were taken for co-rotating and counter-rotating propellers, examining two center-to-center separation distances under two advance ratios of 0 and 0.47. The key findings revealed a significant correlation between noise reduction and increasing relative phase angle, particularly at 90°, across all directivity angles and regardless of propeller rotation direction, advance ratio, and separation distance. The results illustrated significant reductions in noise directivity and tonal noise at the blade pass frequency. The experimental results also revealed that phase synchronization offers a slight advantage for co-rotating propellers over counter-rotating propellers at an advance ratio of 0.47. The separation distance between the two propellers appears to have a minimal impact on the noise level at the first blade pass frequency using the phase synchronization method. Finally, the experiments demonstrated that phase synchronization can provide significant benefits in noise control for DEP configuration.

Nomenclature

c	=	wing chord [m]
C_T	=	coefficient of thrust [-]
n	=	the rotational speed in revolution per second
BPF	=	blade passing frequency [Hz]
V	=	free stream velocity [m/s]
D	=	propeller diameter [inch]
f	=	frequency [Hz]
J	=	advance ratio [-]
L	=	wing span [m]
N_b	=	the number of blades
$OASPL$	=	overall sound pressure level [dB]
P	=	propeller pitch [inch]
P/D	=	propeller pitch to diameter ratio [-]
p_{ref}	=	reference acoustic pressure [μPa]
rpm	=	revolutions per minute [-]

*Research Associate, Department of Aerospace Engineering, University of Bristol, en22804@bristol.ac.uk, AIAA member (****).
†Research Associate, Department of Aerospace Engineering, University of Bristol, AIAA member (****).
‡Research Associate, Department of Aerospace Engineering, University of Bristol, AIAA member (****).
§Senior Lecturer, Department of Aerospace Engineering, University of Bristol.
¶Professor of Aerodynamics and Aeroacoustics, Department of Aerospace Engineering, University of Bristol.

s	=	center-to-center-distance [mm]
SPL	=	sound pressure level [dB]
t	=	time [s]
V	=	free-stream inflow velocity [m/s]
ψ	=	phase angle [deg]
θ	=	observer angle [deg]
ω	=	rotation speed in revolutions per minute
ϕ_{PP}	=	power spectral density (dB/Hz)

I. Introduction

The rapid development of urban air mobility (UAM) reflects a profound shift towards more sustainable and efficient urban transportation, motivated by innovations in battery technology, distributed electric propulsion (DEP), and autonomous systems [1, 2]. This evolution is marked by the development of advanced vertical takeoff and landing (VTOL) vehicles, designed to operate in urban areas for a variety of applications, including passenger transport, logistics, and emergency services [3]. However, these advancements bring challenges, notably noise pollution in densely populated areas, a critical concern that could impede the broader adoption of UAM technologies [4]. The growing use of multi-rotor aircraft for civilian and military purposes further emphasizes the need for solutions to mitigate rotor noise, a pervasive issue for communities surrounding urban environments [5, 6].

Amid these challenges, the concept of DEP emerges as a promising solution, offering enhanced propulsive efficiency and the potential for reduced noise levels [7]. DEP's innovative approach to distributing thrust across multiple motors allows for not only improved aerodynamics but also opens up new possibilities for quieter, more environmentally friendly VTOL designs [8]. This concept is now at the forefront of research across government, industry, and academic circles, aiming to address the dual challenges of efficiency and noise pollution in urban air mobility [9].

In DEP configurations, the mechanisms responsible for noise generation can be categorized into tonal noise at multiples of the Blade Passing Frequency (BPF) (propeller-propeller [10]/-pylon [11]/-wing [12, 13] interaction noise, propeller steady and unsteady loading noise and thickness noise [14, 15]) and broadband noise (turbulence-ingestion noise [16, 17] and trailing-edge noise). Extensive experimental research has focused on hover and forward flight configurations to explore the impact of propeller design, including blade tip speed, blade pitch, blade radius, chord, twist, and the number of blades on performance trends [18, 19]. The experimental data were meticulously analyzed to enhance propeller performance and identify key aerodynamic metrics such as thrust, drag, efficiency, and the effects of Reynolds number for aerodynamic scaling [20]. Moreover, comprehensive acoustic and aerodynamic evaluations were performed to measure aerodynamic loads and far-field noise radiation, considering edgewise flow conditions [21] and turbulent flow [22]. Therefore, identifying and implementing effective methods to control and mitigate these types of noise is not only a matter of scientific interest but also of substantial practical importance, highlighting the need for targeted noise reduction strategies in the advancement of DEP systems. In this context, recent advancements have led to the categorization of noise control techniques for multi-rotor aircraft into passive and active control. Passive control strategies are primarily concerned with the rotor blade's design optimization, including modifications in blade shape, trailing edge, and airfoil distribution [23–25]. Conversely, active control methods, such as Active Noise Cancellation (ANC), employ the generation of an antinoise—a sound wave with equal amplitude but in the opposite phase to the unwanted noise—to effectively neutralize it [26]. Expanding on active approaches, synchronization of acoustic sources in multi-propeller aircraft presents a novel approach [27–29]. This method involves modifying the relative phase of synchronized rotors to manage the noise directionality, enabling focused noise suppression. Such synchronous control techniques prove particularly efficacious in multi-rotor configurations, offering a technique for reducing noise in DEP applications.

Related studies have demonstrated the potential of propeller phase control to modify acoustic characteristics, especially at low frequencies. Notable research includes Pascioni et al. [27], who achieved a 6 dB reduction in the BPF for 3-bladed propellers, and a numerical study by Pascioni and Rizzi [30] showing a 20 dB reduction in BPF noise using 2-bladed propellers, at an advance ratio of $J = 0.60$. Zhou and Fattah [31] noted that the sound emissions from two propellers can vary by up to 10 dB, depending on their relative phase angle. Schiller et al. [32] implemented the phase control technique both in experiments and theoretical models under static thrust conditions, showing that adjusting the relative phase angle could lead to a sound pressure level (SPL) reduction at the first BPF by about $4 - 5$ dB. Furthermore, Hertzman et al. [33] provided experimental evidence that operating propellers with a relative phase angle of 90 degrees, in a static condition (i.e no inflow) and at a rotational speed of 3000 rpm, was capable of achieving an SPL reduction

of up to 8 dB at the BPF. Recently, Turhan et al. [34] investigated the noise suppression capabilities of DEP systems examining their performance in both static thrust and inflow conditions via electronic propeller synchronization. This study highlighted notable decreases in both noise directivity and tonal noise at the first BPF. A relative phase angle of $\Delta\psi = 90°$ demonstrated the maximum noise reduction, showing an 8 dB reduction at the first BPF and a 2 dB reduction in overall sound pressure level (OASPL) under static thrust condition ($J = 0$). For in-flow conditions ($J > 0$), the same phase angle led to a remarkable reduction of approximately 24 dB at the first BPF and 6 dB in OASPL, compared to $\Delta\psi = 0°$.

This study focuses on the tonal noise generated by two adjacent propellers in a DEP configuration, aiming to understand how noise levels are affected by the separation between the propellers and the phase angle difference between them. It further examines the influence of propeller rotation direction—testing both co-rotating and counter-rotating configurations—on noise attenuation in static thrust and inflow conditions. Furthermore, the research uniquely investigates the experimentally unexplored impact of phase locking under conditions of non-zero inflow speed (i.e., advance ratio > 0), by varying separation and rotational directions. This analysis allows us to explore noise suppression in DEP systems by identifying the optimum relative phase angle between propellers, to achieve the lowest noise level, for operating in forward flight conditions with different design configurations. The structure of this paper is as follows: Section II briefly describes the experimental setup and test matrix. In Section III, experimental data are analyzed in detail, and the effectiveness of the phase synchronization method is verified. Finally, Section IV summarizes the study.

II. Methodology

To investigate the effects of propeller-propeller interaction on noise attenuation, the experimental assessments were performed using two adjacent propellers at advance ratios of $J = 0$ and 0.47, using seven relative phase differences from $\Delta\psi = 0°$ to 90°. $J = 0.47$ was selected as one of the advance ratios for the experiments due to its optimal operational efficiency. At this ratio, the propeller not only operates with high efficiency but also exhibits a relatively high thrust coefficient (C_T), making it ideal for assessing the impact of the DEP configuration on noise attenuation. The tests were conducted for propellers in both co-rotating and counter-rotating configurations. The separation between the two propellers was varied between 1% and 5% or the propeller diameter.

All the measurements presented in this study were conducted at the aeroacoustic facility located in the wind tunnel laboratory at the University of Bristol [35]. This facility comprises a temperature-controlled, closed-circuit, open-jet anechoic wind tunnel. The anechoic room's exposed surfaces, including the anechoic chamber and contraction nozzle, are either acoustically lined or covered in acoustic foam wedges to absorb any sound reflections completely. The anechoic chamber is capable of providing anechoic measurements down to 160 Hz, in accordance with the ISO 3745 standardized testing procedure for both pure tone and broadband testing. Airflow is supplied by a 55 kW centrifugal fan through a series of silencers and ducts, then homogenized by mesh grids and a honeycomb section for consistent flow. The wind tunnel's exit nozzle, with dimensions of 0.5 m by 0.775 m and a contraction ratio of 8.4, facilitates stable airflow speeds between $5m/s$ and $40m/s$, with a turbulent intensity of approximately 0.2% in an anechoic environment [35].

The experimental setup, illustrated in Fig.1, comprises two propulsion units with propellers mounted on a wing, representative of a DEP configuration. A far-field microphone array was positioned so that the microphone at $\theta = 90°$ was located 1.75 m directly above the wing's center, equidistant from both propellers. The microphone array consisted of 23 G.R.A.S 40PL microphones, each 1/4 inch in diameter, arranged at 5° intervals spanning polar angles from 30° to 130°. These microphones cover a frequency spectrum from $f = 10$ Hz to 20 kHz, with dynamic ranges up to 142 dB and precision of ±1 dB. Data collection was conducted at a sampling rate of 2^{16}Hz and a measurement time of $t = 40$ s. The power spectra of the collected data were analyzed using the MATLAB Pwelch method [36], with the results presented at a frequency resolution of 1 Hz.

The experiments were performed using a set of two-bladed carbon fiber propellers, each with a diameter of $D = 9$" and a pitch of $P = 5$", arranged in a co-rotating and contra-rotating configuration. The wing was designed using a NACA0018 profile, with a chord of $c = 0.3$ m and a span of $L = 0.94$ m. It was fabricated from a 6000 series aluminum alloy. The propellers were positioned 150 mm from the wing's trailing edge to the propeller's leading edge, and roughly 0.5 m from the nozzle exit, as is normal with the tunnel free-stream flow. Each propeller in the setup is powered by a 540kV AT4125 T-motor, with a maximum continuous output of 2.2 kW. To track the phase angle of the propeller blades with high precision, a 12-bit RLS® RE36IC incremental output encoder is employed, with an accuracy of ±0.3°. The propellers' relative phase angles are managed through a specialized system that issues two distinct signals for different purposes: the first signal is utilized by the motor control software to regulate the propellers' relative phase angles, while the second signal is directed to a Tektronix TBS1102C oscilloscope, enabling real-time monitoring of

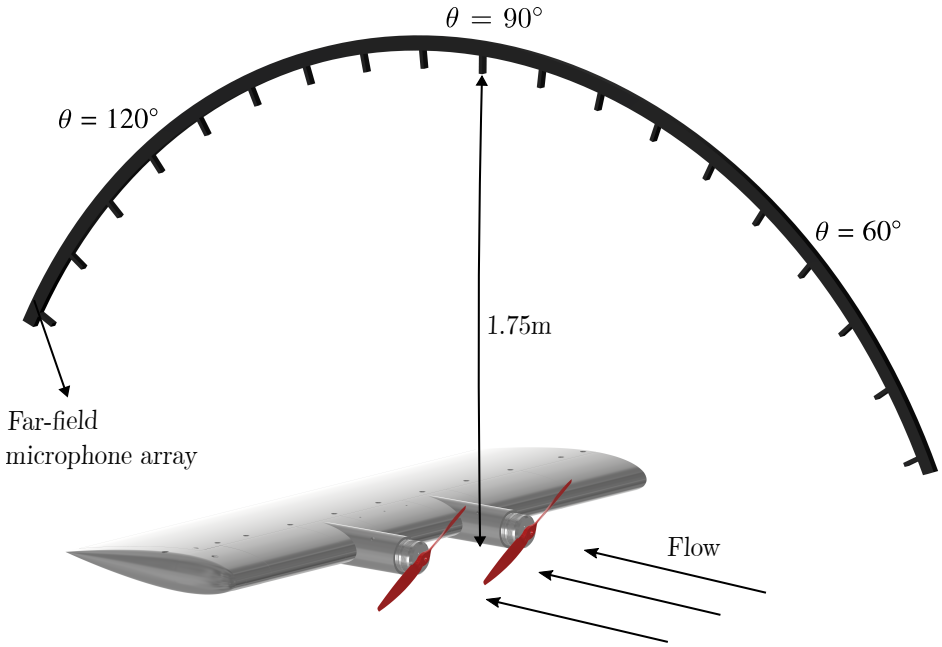

Fig. 1 Schematic representation of the experimental setup.

any changes in phase angle during tests. Additionally, Tektronix electric voltage probes are connected to capture the position signal, generated by the controller after processing pulses from the position encoder. Operating at a speed of 5000 rpm, the setup maintains a positional error consistently below 1°, and the peak-to-peak speed error is kept under 0.05% (2.5 rpm) [34].

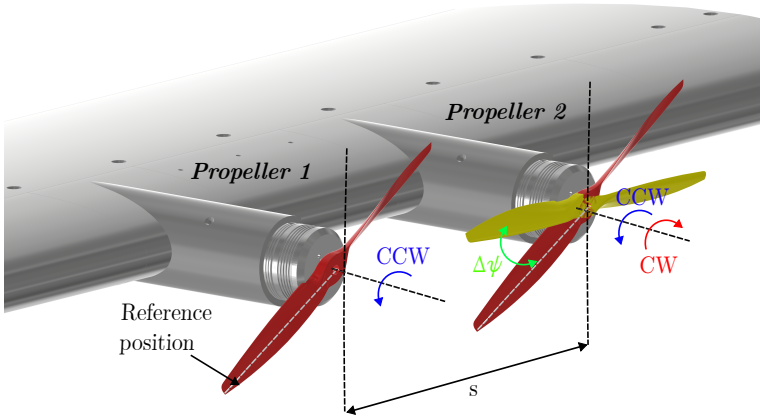

Fig. 2 Relative phase synchronization for the two-propeller configuration.

Figure 2 presents the definition of the relative phase angle ($\Delta\psi$) for the two-propeller systems and the other geometric parameters of the experimental setup. The center-to-center distance between the propellers in the experimental setup was achieved by strategically adjusting the positioning of the propulsion units using spacers, which were placed between the two propulsion units on the leading edge of the wing. By altering the spacing between the propellers, the separation distance could be effectively changed, allowing for different configurations to be tested. Throughout the study, the separation distance between the propellers was systematically varied between $s/D = 1.01$ and 1.05, where s represents the center-to-center distance and D is the propeller diameter. The relative phase angle is defined by the angular difference between the blades of the two propellers. To establish a baseline, the propellers were initially aligned horizontally along the wing span, setting the initial relative phase difference at $\Delta\psi = 0°$. Propeller 1 was identified as the main

propeller, rotating counterclockwise, with its initial phase maintained at a phase angle of $\psi = 0°$. Propeller 2, referred to as the slave propeller, rotates counterclockwise under co-rotation configuration, and clockwise under counter-rotation configuration. The blade position on Propeller 2 was then adjusted to achieve various relative phase angles and rotation directions, while Propeller 1 was kept in its original position and rotation direction. This study investigated seven different relative phase angles ($\Delta\psi$) ranging from 0° to 90° in increments of 15°.

The aeroacoustic measurements were conducted at a wind tunnel velocity of 0 and 9 m/s, corresponding to advance ratios of $J = 0$ (indicating static trust condition) and $J = 0.47$, respectively, at the propellers rotating at a speed of 5000 rpm. The advance ratio is a non-dimensional term defined as:

$$J = \frac{V}{nD} \tag{1}$$

where V is the free-stream inflow velocity in m/s, n the rotational speed in revolution per second, and D is the propeller diameter in meters.

III. Results and Discussion

The analysis first examines the impact of the propellers' relative phase angles on far-field noise in both static thrust ($J = 0$) and inflow conditions ($J = 0.47$). Specifically, the study concentrates on the frequency characteristics of these configurations, aiming to explore how the noise can be affected through adjustments in the relative phase angle and alterations in the propellers' separation distance and direction of rotation.

Figure 3 displays the sound pressure level (SPL) across a wide frequency range, observed at an angle of $\theta = 90°$, illustrating the noise spectrum for seven cases of phase angles ($\Delta\psi$) at an advance ratio of $J = 0$ (static thrust condition) and center-to-center distance of $s/D = 1.01$. These figures compare the SPL under two propeller conditions: co-rotating and counter-rotating. The SPL was calculated using the following equation:

$$SPL = 10 \cdot \log_{10}\left(\frac{\phi_{pp}}{p_{ref}^2}\right), \tag{2}$$

where ϕ_{pp} represents the power spectral density of the measured acoustic pressure, and p_{ref} is the reference acoustic pressure (equal to 20 μPa). Overall, the findings indicate that adjusting the blade's relative phase angle ($\Delta\psi$) does not markedly affect the levels of broadband noise, consistent with conclusions drawn in earlier research [32, 34, 37]. In Figs. 3(a) and (c), the motor mechanical noise is represented by a dashed light grey line. This noise is characterized by specific tones superimposed on a broader spectrum of broadband noise. Notably, the noise generated by the propeller's aerodynamics exceeds the motor's mechanical noise by more than 15 dB. This significant difference indicates that the motor noise plays a minor role in the overall acoustic profile, confirming that the aerodynamic noise from the propeller is the dominant factor in the acoustic readings captured by the far-field microphone array. The tonal noise is recognized as the first BPF, occurring at a frequency of 166.6 Hz, accompanied by its harmonics that appear with each propeller rotation. The first BPF was calculated using the following equation:

$$BPF = \frac{\omega N_b}{60}, \tag{3}$$

where ω is the rotation speed in revolutions per minute and N_b is the number of blades.

As shown in Figs. 3(a) and (c), the peak amplitudes of these harmonic frequencies are significantly lower than that of the first BPF. The results of the first blade pass frequency ($f/BPF = 1$) were magnified, and presented on the side of noise spectra, for comparison. The data presented in Figs.3(c) and (d) show that at a relative phase of $\Delta\psi = 0°$, the amplitude of the first BPF remains almost the same in both co-rotating and counter-rotating conditions. An increase in the relative phase to $\Delta\psi = 45°$ leads to a slight reduction in the noise levels at the first BPF. Further increasing the relative phase angle to $\Delta\psi = 90°$ results in a distinct change in the noise signature at the BPF. For the relative phase of $\Delta\psi = 90°$, the noise level of the first BPF for co-rotating and counter-rotating two-propellers is found to be approximately 11 dB and 10 dB lower, respectively, compared to the relative phase of $\Delta\psi = 0°$.

Figure 4 provides a detailed comparison of the far-field noise directivity at the first BPF across a range of directivity angles, covering seven relative phase angles. This analysis encompasses conditions of $J = 0$ and 0.47, for both co-rotating and counter-rotating propellers, with a center-to-center distance of $s/D = 1.01$. Overall, a significant reduction in the first BPF noise is observed as the relative phase angle increases, regardless of the advance ratio. Across

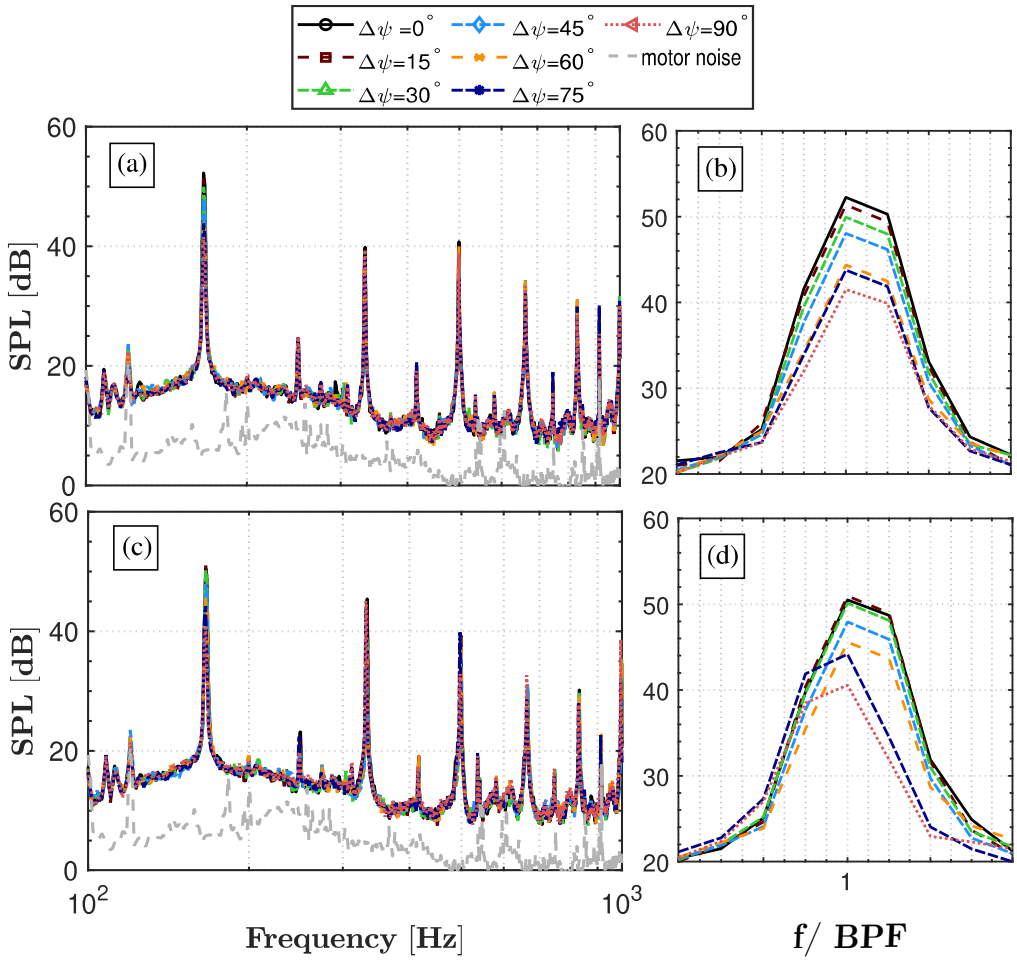

Fig. 3 Frequency characteristics of two 2-bladed propellers with seven relative phase angles at an observer angle of $\theta = 90°$ and center-to-center distance $s/D = 1.01$, for an advance ratio of $J = 0$ (static thrust condition), (a) noise spectra for co-rotating configuration, (b) the first BPF tones for co-rotating configuration, (c) noise spectra for counter-rotating configuration and (d) the first BPF tones for counter-rotating configuration.

all directivity angles and advance ratios, the lowest noise level is consistently achieved at a relative phase of $\Delta\psi = 90°$, irrespective of the directivity angle or advance ratio. These results also demonstrate that introducing inflow enhances the effectiveness of noise reduction achieved through blade synchronization.

Figures 4(a)-(b) present the variations in noise at the first BPF as a function of the directivity angle (θ) at $J = 0$. This represents static thrust conditions, for co-rotating and counter-rotating configurations, respectively. Upon comparing the results across seven relative phase angles, it is observed that for a relative phase difference of $\Delta\psi =< 45°$, there is no substantial difference in noise reduction between the two rotational configurations. However, for $\Delta\psi = 90°$, the magnitude of the first BPF in the upstream region ($\theta < 85°$) shows an approximate disparity of ≈ 5 dB between co-rotating and counter-rotating blades. The results for propellers operating with an inflow condition, corresponding to advance ratios of $J = 0.47$, are presented in Figs. 4(c)-(d). While these results exhibit a trend similar to that of $J = 0$, the noise reductions achieved due to propellers' phase synchronization are considerably more pronounced. Increasing the relative phase of the propellers leads to a substantial and ongoing decrease in noise levels. Notably, significant noise reductions for the inflow condition are achieved at $\Delta\psi = 75°$ and $\Delta\psi = 90°$. In line with earlier findings reported in the literature [32, 34, 37, 38], the optimal relative phase offset for 2-bladed rotors is consistently $\Delta\psi = 90°$, irrespective of flow conditions and rotation direction.

Figure 5 provides a comparison of the SPL directivity patterns at the first BPF for co- and counter-rotating propellers at a center-to-center distance of $s/D = 1.01$. The patterns are plotted across a range of directivity angles (θ) and consider three relative phase angles ($\Delta\psi = 0°, 75°$ and $90°$). The plots for two advance ratios, $J = 0$ and $J = 0.47$, are

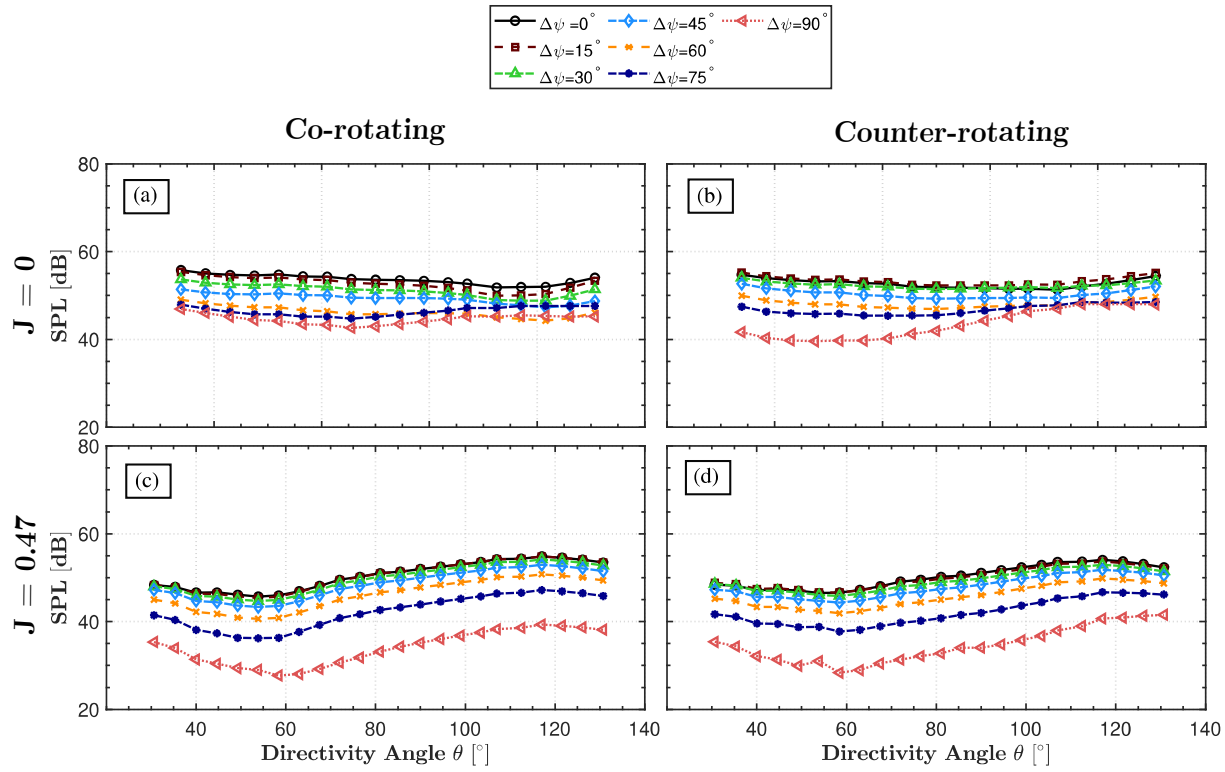

Fig. 4 Comparison of the SPL directivity pattern at the first BPF for two advance ratios at centre-to-centre distance $s/D = 1.01$, for co-rotating and counter-rotating configurations (a) $J = 0$ for co-rotating blades, (b) $J = 0$ for counter-rotating blades, (c) $J = 0.47$ for co-rotating blades and (d) $J = 0.47$ for counter-rotating blades.

shown in Figs. 5(a) and (b), respectively. For both co- and counter-rotating cases at $J = 0$, the SPL tends to remain the same regardless of the directivity angle when the relative phase angles are set to $\Delta\psi = 0°$ and 75°. A similar consistency is observed at $J = 0.47$ for the same relative phases, yet the levels of noise reduction are notably more pronounced, suggesting an impact of the inflow condition on noise directivity. Conversely, the trend for a relative phase of $\Delta\psi = 90°$ appears to be influenced by the rotation direction across both advance ratios.

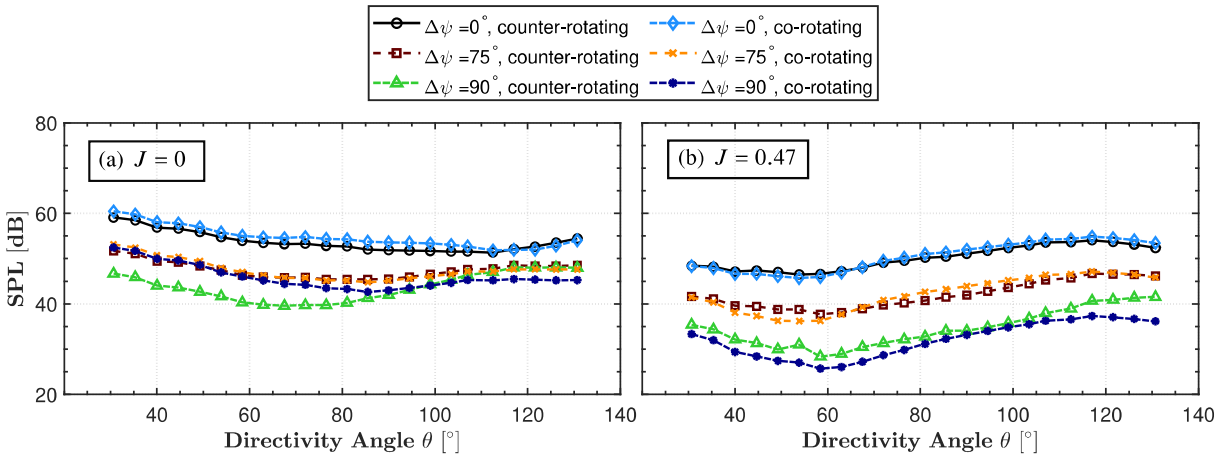

Fig. 5 Comparison of the directivity pattern of a sound pressure level in dB at the first BPF at center-to-center distance $s/D = 1.01$ for co- and counter-rotating propellers, considering three relative phase angles, $\Delta\psi = 0°, 75°$ and 90° (a) $J = 0$, (b) $J = 0.47$.

Figure 6 shows the ΔSPL variation, which is the change in SPL behavior between the relative phase difference of $\Delta\psi = 90°$ and the reference case of $\Delta\psi = 0°$. This change is examined across the directivity angles for both co-rotating and counter-rotating configurations at the two advance ratios, $J = 0$ and $J = 0.47$. The ΔSPL for the static thrust condition ($J = 0$) indicates a noise reduction of approximately 10 dB at the observer location of $\theta = 85°$ for both directions of rotation. However, at observer locations with $\theta < 85°$, the counter-rotating configuration demonstrates a higher noise reduction compared to the co-rotating case, with a difference of about 5 dB. Conversely, for $\theta > 85°$, the co-rotating configuration exhibits a 2.5dB higher noise reduction compared to the counter-rotating case. This finding is particularly intriguing since previous literature has suggested that co-rotating rotors might offer more significant noise reduction benefits than counter-rotating rotors [32]. Additionally, it was noted that the predicted change in sound power for counter-rotating rotors needs experimental validation. According to this study, the direction of rotation, depending on the directivity angle, plays a crucial role in noise reduction at the first BPF under static thrust conditions ($J = 0$). As seen in Fig. 6, the introduction of inflow has a substantial impact on noise reduction levels. With inflow, noise reduction reaches up to 19 dB, with co-rotating propellers offering more potential benefits than counter-rotating propellers.

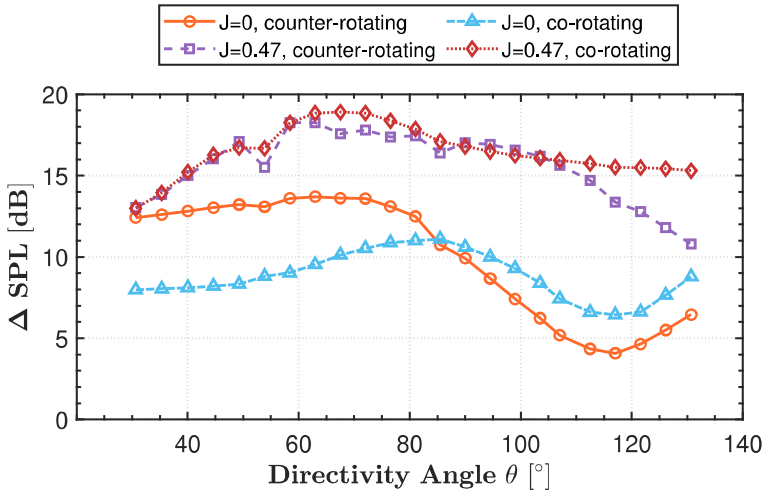

Fig. 6 Comparison of ΔSPL variation between $\Delta\psi = 90°$ and the propeller reference configuration ($\Delta\psi = 0°$) across directivity angles for both configurations at two advance ratios, $J = 0$ and 0.47.

A. Effects of the separation distance

The influence of the relative phase angle between two propellers and their rotation direction on noise reduction has been discussed in the previous section, for both stationary and inflow conditions. In order to assess whether the separation distance has a significant effect on the noise reduction through the phase synchronization method, Fig. 7 presents the SPL directivity at the first BPF using two center-to-center separation distances, $s/D = 1.01$ and $s/D = 1.05$. These results are shown for two advance ratios: $J = 0$ and $J = 0.47$. In order to better visualize the effect of the separation distance, the results are presented for three different relative phase angles of $\Delta\psi = 0°, 75°$, and $90°$. Generally, the investigation of the SPL directivity at $J = 0$ and 0.47 for both separation distances revealed consistent patterns and trends. Regardless of the separation distance, the shape of the directivity remained unchanged, indicating a similar acoustic behavior at $J = 0.47$ for each respective relative phase angle.

Figure 7(a) presents the first BPF directivity under the static thrust condition, $J = 0$. The noise reduction observed here remains almost the same for the relative phase angles of $\Delta\psi = 75°$ and $90°$, exhibiting minor fluctuations < 1 dB. However, it is crucial to note that the magnitude of the first BPF differs in the upstream region ($\theta < 90°$) between the two separation distances when the relative phase is set at $\Delta\psi = 90°$. Specifically, there exists an approximate ≈ 1 dB disparity in the upstream region between these two separation distances, after which the magnitudes converge and remain consistent, irrespective of separation distance. Similar to the static thrust condition, in the presence of inflow ($J = 0.47$), the noise reduction of the first BPF remains unaffected for both separations for the same relative phase angles, as shown in Fig. 7(b). The results are perfectly matched for each respective relative phase angle. This means the overall noise reduction, in terms of the first BPF noise level, using different center-to-center distances remains unchanged at an advance ratio of $J = 0.47$.

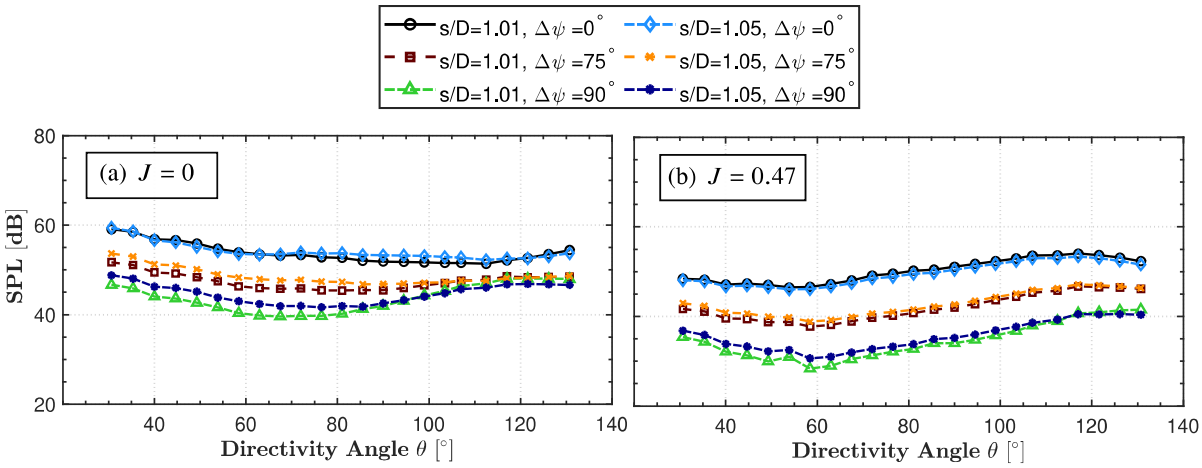

Fig. 7 Comparison of the directivity pattern of a sound pressure level in dB at the first BPF with two separation distances using counter-rotating blades, considering three relative phase angles, $\Delta\psi = 0°, 75°$ and $90°$ (a) $J = 0$, (b) $J = 0.47$.

IV. Conclusion

This study delivers a detailed experimental study of the aeroacoustic properties of a DEP configuration, emphasizing the influence of the relative phase angle between adjacent propellers. The research involved noise measurement for both co-rotating and counter-rotating propellers, focusing on two different center-to-center separation distances under advance ratios of $J = 0$ and 0.47 with a constant propeller rotation rate of 5000 RPM. The results indicate that phase synchronization in DEP systems is a viable method for noise reduction, utilizing the concept of destructive interference within the coherent acoustic source field generated by the propellers.

The acoustic results demonstrate a clear correlation between an increased relative phase angle and noise reduction in the far-field. The most notable acoustic attenuation was observed at a relative phase angle of $\Delta\psi = 90°$, where reductions in the first BPF amplitudes ranged from 15 dB to 19 dB compared to $\Delta\psi = 0°$, depending on the directivity angles. This trend persists irrespective of the propellers' rotation direction, the advance ratio, and the separation distance between them.

The counter-rotating configuration was observed to be more effective at reducing noise—by approximately 5 dB compared to the co-rotating case, up to an observer location of $\theta < 85°$. However, beyond this point, at $\theta > 85°$, the trend reverses, with the co-rotating configuration achieving about 2.5 dB less noise reduction under static thrust conditions. When inflow is considered, phase synchronization proves to be more beneficial, achieving a noise reduction of around 19 dB in the SPL at the first BPF. Co-rotating propellers seem to offer more advantages over counter-rotating propellers in this context. Additionally, the separation distance between propellers had a minimal impact on noise levels at the first blade pass frequency when using the phase synchronization technique.

Declaration of competing interest

The authors declare that they have no known competing financial interests or personal relationships that could have appeared to influence the work reported in this paper.

Data Availability

Data will be made available on request.

Acknowledgement

The authors gratefully acknowledge financial support from the Horizon 2020 research and innovation program (grant agreement number 882842) for the SilentProp project.

Bibliography

[1] Aeronautics, N., "Strategic Implementation Plan 2017 Update," *National Aeronautics and Space Administration, Washington, DC, NP-2017-01-2352-HQ*, 2015.

[2] Commission, E., for Mobility, D.-G., Transport, for Research, D.-G., and Innovation, *Flightpath 2050 – Europe's vision for aviation – Maintaining global leadership and serving society's needs*, Publications Office, 2011. https://doi.org/doi/10.2777/50266.

[3] Kim, H. D., Perry, A. T., and Ansell, P. J., "A review of distributed electric propulsion concepts for air vehicle technology," 2018 AIAA/IEEE Electric Aircraft Technologies Symposium (EATS), 2018, pp. 1–21.

[4] Sahoo, S., Zhao, X., and Kyprianidis, K., "A review of concepts, benefits, and challenges for future electrical propulsion-based aircraft," *Aerospace*, Vol. 7, No. 4, 2020, p. 44.

[5] Ghommam, J., Saad, M., Wright, S., and Zhu, Q. M., "Relay manoeuvre based fixed-time synchronized tracking control for UAV transport system," *Aerospace Science and Technology*, Vol. 103, 2020, p. 105887.

[6] Floreano, D., and Wood, R. J., "Science, technology and the future of small autonomous drones," *nature*, Vol. 521, No. 7553, 2015, pp. 460–466.

[7] Aviation, C., "Strategic Research and Innovation Agenda-The Proposed European Partnership on Clean Aviation," 2020.

[8] Kim, H. D., Perry, A. T., and Ansell, P. J., "A Review of Distributed Electric Propulsion Concepts for Air Vehicle Technology," *2018 AIAA/IEEE Electric Aircraft Technologies Symposium (EATS)*, 2018, pp. 1–21.

[9] Borer, N. K., Patterson, M. D., Viken, J. K., Moore, M. D., Bevirt, J., Stoll, A. M., and Gibson, A. R., *Design and Performance of the NASA SCEPTOR Distributed Electric Propulsion Flight Demonstrator*, 16th AIAA Aviation Technology, Integration, and Operations Conference, 2016, pp. AIAA 2016–3920. https://doi.org/10.2514/6.2016-3920.

[10] Turhan, B., Kamliya Jawahar, H., Bowen, L., Rezgui, D., and Azarpeyvand, M., "Aeroacoustic characteristics of distributed electric propulsion system in forward flight," AIAA AVIATION 2023 Forum, 2023, pp. AIAA 2023–4490.

[11] Block, P., and Gentry Jr, C., "Directivity and Trends of Noise Generated by a Propeller in a Wake," Tech. rep., 1986.

[12] Turhan, B., Jawahar, H. K., Bowen, L., Rezgui, D., and Azarpeyvand, M., "AEROACOUSTIC CHARACTERISTICS OF SINGLE PROPELLER-WING CONFIGURATION," International Institute of Acoustics and Vibration, The 29th International Congress on Sound and Vibration, 2023.

[13] Zhou, W., Ning, Z., Li, H., and Hu, H., "An experimental investigation on rotor-to-rotor interactions of small UAV propellers," 35th AIAA applied aerodynamics conference, 2017, pp. AIAA 2017–3744.

[14] Kim, D. H., Park, C. H., and Moon, Y. J., "Aerodynamic analyses on the steady and unsteady loading-noise sources of drone propellers," *International Journal of Aeronautical and Space Sciences*, Vol. 20, 2019, pp. 611–619.

[15] Turhan, B., Kamliya Jawahar, H., Bowen, L., Rezgui, D., and Azarpeyvand, M., "Turbulent Flow Impact on the Acoustic and Aerodynamic Performance of Overlapping Propellers," 30th AIAA/CEAS Aeroacoustics Conference, 2024.

[16] Bowen, L., Turhan, B., Kamliya Jawahar, H., Rezgui, D., and Azarpeyvand, M., "Aeroacoustic characteristics of distributed electric propulsion configuration with turbulent flows," AIAA AVIATION 2023 Forum, 2023, pp. AIAA 2023–4294.

[17] Hanson, L. P., Baskaran, K., Zang, B., and Azarpeyvand, M., "Aeroacoustic Interactions of a Trailing Edge Mounted Propeller and Flat Plate," *28th AIAA/CEAS Aeroacoustics 2022 Conference*, 2022, p. 2937.

[18] Baskaran, K., Jamaluddin, N. S., Celik, A., Rezgui, D., and Azarpeyvand, M., "Effects of number of blades on propeller noise," *Journal of Sound and Vibration*, Vol. 572, 2024, p. 118176.

[19] Hanson, L. P., Baskaran, K., Pullin, S. F., Zhou, B. Y., Zang, B., and Azarpeyvand, M., "Aeroacoustic and Aerodynamic Characteristics of Propeller Tip Geometries," *28th AIAA/CEAS Aeroacoustics 2022 Conference*, 2022, p. 3075.

[20] Deters, R. W., Ananda Krishnan, G. K., and Selig, M. S., "Reynolds number effects on the performance of small-scale propellers," *32nd AIAA applied aerodynamics conference*, 2014, p. 2151.

[21] Jamaluddin, N. S., Celik, A., Baskaran, K., Rezgui, D., and Azarpeyvand, M., "Aerodynamic noise analysis of tilting rotor in edgewise flow conditions," *Journal of Sound and Vibration*, 2024, p. 118423.

[22] Jamaluddin, N. S., Celik, A., Baskaran, K., Rezgui, D., and Azarpeyvand, M., "Experimental Analysis of Rotor Blade Noise in Edgewise Turbulence," *Aerospace*, Vol. 10, No. 6, 2023.

[23] Zang, B., Hanson, L. P., Stoltz, A., Ho, W. H., Liu, X., and Azarpeyvand, M., "Numerical and experimental investigation of propeller noise with trailing-edge serrations," AIAA AVIATION 2023 Forum, 2023, pp. AIAA 2023–3835.

[24] Hersh, A. S., Soderman, P. T., and Hayden, R. E., "Investigation of acoustic effects of leading-edge serrations on airfoils," *Journal of Aircraft*, Vol. 11, No. 4, 1974, pp. 197–202.

[25] Lee, H. M., Lu, Z., Lim, K. M., Xie, J., and Lee, H. P., "Quieter propeller with serrated trailing edge," *Applied Acoustics*, Vol. 146, 2019, pp. 227–236.

[26] Lueg, P., "Process of silencing sound oscillations," , 1936. US patent 2043416.

[27] Pascioni, K. A., Rizzi, S. A., and Schiller, N., "Noise reduction potential of phase control for distributed propulsion vehicles," AIAA Scitech 2019 Forum, 2019, pp. AIAA 2019–1069.

[28] Patterson, A., Schiller, N. H., Ackerman, K. A., Gahlawat, A., Gregory, I. M., and Hovakimyan, N., "Controller design for propeller phase synchronization with aeroacoustic performance metrics," AIAA Scitech 2020 Forum, 2020, pp. AIAA 2020–1494.

[29] Turhan, B., F. Lopes de M. F., L., F. Pullin, S., Y. Zhou, B., Kamliya Jawahar, H., Gautam, A., Rezgui, D., and Azarpeyvand, M., "Numerical and Experimental Analysis of Synchronized Propellers for Noise Mitigation," 30th AIAA/CEAS Aeroacoustics Conference, 2024.

[30] Pascioni, K., and Rizzi, S. A., "Tonal noise prediction of a distributed propulsion unmanned aerial vehicle," 2018 AIAA/CEAS Aeroacoustics Conference, 2018, pp. AIAA 2018–2951.

[31] Zhou, T., and Fattah, R., "Tonal noise acoustic interaction characteristics of multi-rotor vehicles," 23rd AIAA/CEAS Aeroacoustics Conference, 2017, pp. AIAA 2017–4054.

[32] Schiller, N. H., Pascioni, K. A., and Zawodny, N. S., "Tonal noise control using rotor phase synchronization," Vertical Flight Society Annual Forum and Technology Display (VFS Forum 75), 2019.

[33] Hertzman, O., Fligelman, S., and Stalnov, O., "Abatement of a Multi-Rotor Tonal Noise Component with Phase Control Technology," 28th AIAA/CEAS Aeroacoustics 2022 Conference, 2022, pp. AIAA 2022–2834.

[34] Turhan, B., Kamliya Jawahar, H., Gautam, A., Syed, S., Vakil, G., Rezgui, D., and Azarpeyvand, M., "Acoustic Characteristics of Phase-Synchronized Adjacent Propellers," *The Journal of the Acoustical Society of America*, Vol. accepted, 2024.

[35] Mayer, Y. D., Jawahar, H. K., Szőke, M., Ali, S. A. S., and Azarpeyvand, M., "Design and performance of an aeroacoustic wind tunnel facility at the University of Bristol," *Applied Acoustics*, Vol. 155, 2019, pp. 358–370.

[36] Welch, P., "The use of fast Fourier transform for the estimation of power spectra: a method based on time averaging over short, modified periodograms," *IEEE Transactions on audio and electroacoustics*, Vol. 15, No. 2, 1967, pp. 70–73.

[37] Shao, M., Lu, Y., Xu, X., Guan, S., and Lu, J., "Experimental study on noise reduction of multi-rotor by phase synchronization," *Journal of Sound and Vibration*, Vol. 539, 2022, p. 117199.

[38] Guan, S., Lu, Y., Su, T., and Xu, X., "Noise attenuation of quadrotor using phase synchronization method," *Aerospace Science and Technology*, Vol. 118, 2021, p. 107018.